U. S. Naval Research Laboratory
Washington, DC 20375-5320

NRL/5590/FR--2022/1

Network Topology Control: Traffic Effectiveness, k-Resiliency, and External Constraint Optimization

Joseph Macker, Jeffery W. Weston

Center for Computational Science
Information Technology Division

Clement Kam

Communications and Network Systems Branch
Information Technology Division

December 21, 2022

REPORT DOCUMENTATION PAGE

PLEASE DO NOT RETURN YOUR FORM TO THE ABOVE ORGANIZATION

1. REPORT DATE	**2. REPORT TYPE**	**3. DATES COVERED**	
		START DATE	**END DATE**
December 21, 2022	NRL Formal Report	September 2020	September 2022

4. TITLE AND SUBTITLE
Network Topology Control: Traffic Effectiveness, k-Resiliency, and External Constraint Optimization

5a. CONTRACT NUMBER	**5b. GRANT NUMBER**	**5c. PROGRAM ELEMENT NUMBER**
		61153N
5d. PROJECT NUMBER	**5e. TASK NUMBER**	**5f. WORK UNIT NUMBER**
		1P81

6. AUTHOR(S)
Joseph Macker, Jeffery W. Weston, Clement Kam

7. PERFORMING ORGANIZATION / AFFILIATION NAME(S) AND ADDRESS(ES)	**8. PERFORMING ORGANIZATION REPORT NUMBER**
U. S. Naval Research Laboratory 4555 Overlook Ave SW, Washington, DC 20375-5320	NRL/5590/FR--2022/1

9. SPONSORING / MONITORING AGENCY NAME(S) AND ADDRESS(ES)	**10. SPONSOR / MONITOR'S ACRONYM(S)**	**11. SPONSOR / MONITOR'S REPORT NUMBER(S)**
Office of Naval Research One Liberty Center 875 N. Randolph Street, Suite 1425 Arlington, VA 22203-1995	ONR	

12. DISTRIBUTION / AVAILABILITY STATEMENT
DISTRIBUTION STATEMENT A: Approved for public release, distribution is unlimited

13. SUPPLEMENTAL NOTES

14. ABSTRACT
In this report, we summarize research into wireless network topology control to manage interference produced by the network while also improving resiliency and traffic efficiency. In past work, topology control solutions largely focused on optimal energy conservation, but such solutions result in poor traffic performance and fragility due to the sparse connections. Past solutions also do not focus on external interference constraints, multicast communications, or significant network heterogeneity. To address these shortcomings, this project investigated and developed solutions to quantitatively adapt resiliency while managing complex operating constraints and varying network traffic and routing types. Network connection resilience impacts network data transport in complex ways, so traffic effectiveness is examined by this effort in both simulation and emulation. We demonstrate that small increases in connectivity can lead to dramatic improvements in traffic delivery effectiveness. Work to be presented covers topology control designs, constraint-based models, and connected dominating set (CDS) topology approaches to minimize additive transmission energy impacting external location along with experimentation of expected network performance under both static and dynamic conditions.

15. SUBJECT TERMS

16. SECURITY CLASSIFICATION OF:			**17. LIMITATION OF ABSTRACT**	**18. NUMBER OF PAGES**
a. REPORT	**b. ABSTRACT**	**c. THIS PAGE**		
U/U	U/U	U/U	SAR	30

19a. NAME OF RESPONSIBLE PERSON	**19b. PHONE NUMBER** *(Include area code)*
Joseph P. Macker	(202)-302-7552

This page intentionally left blank

CONTENTS

FIGURES

EXECUTIVE SUMMARY

Dynamic network topology control is a fundamental problem in wireless communication networks and is especially useful for constructing and maintaining networks with desirable properties. Performing effective topology control and reducing overall network node transmission power requirements can improve a wireless networked system in many ways, including the following: reducing network self interference and contention, reducing external radio interference and detection probability, optimizing the network structure to take advantage of platform and environment heterogeneity, and lastly, it may reduce energy consumption of platforms that operate on limited power or batteries. Naive approaches to wireless topology control have also been shown to have potentially detrimental performance effects, including reduced network traffic load capacity, increased information loss, increased network delay, and increased fragility of the network to dynamics and disruption. Although wireless network topology control has been studied over the past two or so decades, much of the past work has concentrated on optimizing energy consumption of the network in terms of battery limitations and does not consider the complex system-level trade-offs resulting from contention and operational fragility. In addition, minimal progress has been made in considering primary external constraints such as reducing detectability and minimizing interference caused by distributed network transmissions.

Much of the previous foundational topology control work in wireless sensor networks (WSNs) has relied on simplified geometric assumptions, producing ineffective solutions to resolve the effects of more complex signal propagation, external interference and detection, and heterogeneous nodal characteristics. Optimal theoretical solutions to topology control in networks, such as the minimum spanning tree (MST), result in large network diameters and sparse connections, leading to significant congestion, delay, and fragility to dynamics in real-world wireless networks. To address these issues, we present and evaluate approaches balancing the formation of resilient structures against the competing requirement of reducing network transmission power requirements using a constraint-based model. As we will show, adding connection resiliency in the topology control process protects against network failures and dynamics but also significantly increases the traffic capacity within a network, so it is a highly desirable feature.

This page intentionally left blank

NETWORK TOPOLOGY CONTROL: TRAFFIC EFFECTIVENESS, k-RESILIENCY, AND EXTERNAL CONSTRAINT OPTIMIZATION

1. OVERVIEW

1.1 Introduction

This paper summarizes research and development performed to develop fundamental wireless network topology control and scheduling mechanisms to optimize network transmission requirements in mobile ad hoc networks (MANETs). As an example, we develop adaptive algorithms to minimize accumulative required transmit power in connected multihop wireless networks by targeting topology optimization and optimal routing/scheduling subject to an external received network energy constraint. We also develop and study k-resilient network topology control algorithms that manage the resultant structural integrity of the network while providing increases in network traffic delivery effectiveness. Using both static and mobile network simulation models, we demonstrate increased communication network resilience to dynamics and failures and improvements in network traffic delivery statistics.

This paper builds from two previously published NRL formal reports [1, 2] that provide more detailed background on the problem and the technical approach and present early analytic results related to a variety of algorithms and problem scenarios.

In [2], we consider a case where the interference caused by the operating wireless network at some external location is constrained by some power threshold, while at the same time, we maintain a goal of connecting the wireless communication network using as many nodes as possible to form a tree without exceeding the defined threshold. In this formulation, the cost to connect a pair of nodes is the sum of the interference caused by transmitting in each direction. We call this the *largest constrained tree* (LCT) problem. At a fundamental level, we first proved that this problem is nondeterministic polynomial-time (NP) complete, and then we formulated it as a mixed integer linear program to be solved computationally. We consider two different cost metrics, one for the cases where there is information about the external node(s) location and one for where there is not. We generate Monte Carlo simulation results for many different network setting parameters, which serve to characterize the performance of our algorithm in different scenarios. As expected, we observed that larger networks can be constructed with higher node density, farther external node distance, and lower network activity levels.

In [1], we build off applied graph theory approaches and metrics and develop a topology control framework and analytic model that allows a wireless network to optimize its topology against generic operational constraints. The approach supports complex propagation models while targeting the minimization of the maximum transmit power required of individual transmitters used within the network. In this approach, we include efficient support for multicast group communications in the formulation. We further adapt and extend this design approach to support k-resilient topology construction. We then evaluate the efficiency and resiliency of a unicast and multicast k-resilient topology algorithm against other basic fundamental topology

Manuscript approved December 20, 2022.

control approaches using analytic network models. We conclude that the k-resilient protocol framework provides a basic design suitable for ad hoc wireless topology control by balancing the minimization of maximum transmission power used within an ad hoc network against competing resiliency requirements. In [1], we also provide appendices documenting the software models and algorithms developed in detail.

In this paper, we summarize more recent technical research project developments and simulations since [1, 2]. As a reader, please consult those previous reports, if needed, for additional background, initial design details, and an overview of constraint-based modeling.

The paper is organized as follows. First, we briefly review past work and discuss our unique contributions and designs. Second, we present our wireless ad hoc network simulation models using the network simulator version 3 (ns3) and we discuss k-resilient topology control experimental results examining the trade-offs associated with network traffic effectiveness across a series of randomized-but-static wireless network experiments. Third, we present similar results for a series of randomized dynamic MANET trials under various levels of topological resilience examining both wireless link fading and network mobility scenarios using the network emulator the Extendable Mobile Ad hoc Network Emulator (EMANE). Fourth, we present new fundamental design work on a tiered backbone approach to topology control and scheduling using the concept of a connected dominating set (CDS) and examine its performance with external network constraint models. We conclude with a brief discussion of ongoing challenges and future planned work.

1.2 Related Past Work and Motivation

As mentioned in Section 1.1, see [1, 2] for a more extensive discussion of technical background, past related optimal graph theory work, and early developments and analyses of both adjustable resilient topology control and the LCT optimization problems. This report mainly focuses on the impact of topological resilience levels on overall network traffic flow delivery of the network while also presenting new theoretical designs and evaluation of a two-tiered topology control model based upon the concept of the CDS. While we refer the reader to past published reports for more background detail, we will briefly outline some of the key characteristics and analysis relevant to military wireless networks distinguishing this work from past work and putting the discussed research in a tactical wireless network context. Table 1 summarizes the relevance and primary focus of this work.

Table 1—Relevance of This Work

	Past work	Present work
Platform environment assumptions	homogeneous	heterogeneous
Propagation assumptions	often distance correlated	complex models supported
User traffic and routing	unicast centric	unicast and multicast
Topology optimization goals	internal minimal cost, sparse connections	adjustable k-resilient connections, minimal cost with more generalized constraints, extended optimization to external constraints

Past work on wireless topology control has mainly focused on wireless sensor networks (WSN) and has often targeted minimizing network connections and conserving network energy as goals. The bulk

of these designs are not sufficient for more general use cases and Table 1 lists some of the capabilities relevant to military wireless network environments that are being addressed in our present work to make topology control designs more generally effective and useful. First, the design models we have developed support a distributed network consisting of heterogeneous platforms where each platform may have unique properties and constraints. Such heterogeneity can include a mixture of directive antennae, mobility, and power constraints that differ amongst deployed platforms within an actual network. Second, radio frequency (RF) propagation models are often abstracted in past work on topology control for WSNs, with geometric distance assumptions often being made [1]. However, as shown in [1], realistic operational environments present reliable connection-cost relationships that are not always distance correlated (e.g., terrain propagation, selective fading). Third, unlike commercial data networks, military tactical networks often need to directly support efficient group traffic delivery, and so an evaluation of group-centric network communications, or multicast network traffic transport, becomes essential to address. Our resilient topology control designs and network simulation studies include multicast routing and transport considerations. Lastly, topology optimization in past work largely targets optimization of internal operational constraints, such as minimal energy consumption of the network. Our newer work develops a topology control design that adapts to more complex, external network constraints, such as minimizing external interference caused by network operations at some location or reducing the detection probability given a certain constraint model.

1.3 Review of Project Designs and Concepts

To review, in [2], we concentrate on studying the LCT problem and develop numerical simulations to examine effectiveness against external constraints. We represent the network and the candidate links as a complete graph with costs defined by the power received by a node external to the main network when the link is closed, accounting for path loss. The LCT problem is formally defined in terms of the network graph as the largest connected component of the graph such that the sum of the chosen link costs is below a threshold, representing the sensitivity of the external node to the cumulative power emitted by the main network. With this model and formulation, we proved that the LCT problem is NP-complete via reduction from the vertex cover problem. Then we formulated the LCT problem as a mixed integer linear program (MILP) that is polynomial in the number of constraints. Using an open-source solver, we simulated the LCT problem, and a comparison of the computation time against a brute force method showed that the required time increases with the network size at a slower rate for the MILP approach. Additionally, numerous simulations were run to characterize the average maximum tree size for various network scenarios, and the results suggest that increasing the node density or reducing network activity are ways to increase the tree size within the sum power constraint.

In [1], we address the topology control problem of achieving a maximum minimum transmit power (MMTP) solution for each wireless network transmission link. The minimum transmit power (MTP) needed to reach each topology neighbor is calculated under the constraint of maintaining a reliable connected topology and additionally may include other external constraints (e.g., minimizing external interference). The maximum of these MTPs is used in the localized neighborhood of the topology to support efficient multicast to all direct neighbors in the resultant topology result. Since achieving efficient network group communications is a key factor in effective tactical network design, this is one of that factors that distinguishes our approach from previous work. We also contrast our present work to previous optimal theoretical work that only addresses the minimization of required network connections, and we demonstrate that such past approaches result in poor traffic delivery and network fragility under operational dynamics. In summary, we develop and study a general constraint approach to topology control including an adaptable k-resilience capability. Our work is partially based on work originally done in [3], where the author demonstrated good graph spanning and

degree properties of a topology control algorithm called X topology control (XTC). The XTC approach is adaptable to distributed, autonomous operation while remaining agnostic to distance properties of the graph edges within the network. Such properties form a solid design foundation on which to build a topology control approach in complex wireless network environments by supporting topology calculations that meet generic cost constraints. In [1], we implemented a model of a k-resilient XTC extension based upon original work done in [4]. We developed an ability to utilize generic edge cost constraints during the construction phase and we refer to this algorithm implementation as kXTC, where kXTC is equivalent to the original XTC topology result when $k = 1$. kXTC guarantees that a network of minimum k-connectivity will be constructed, if possible, where k equals the minimum number of edges that must be removed to disconnect the resultant network communication graph G formed by the algorithm. This adaptive k-resilient lower bound is a property examined further throughout the randomized MMTP network scenario simulations and emulations included in this report.

Our previous work [1] explored the graph theoretic and power reduction characteristics exhibited by kXTC when modeling communication link cost as the minimum transmit power required to establish reliable communication links to candidate network neighbors. As an example, Table 2 shows resulting average MMTP profiles for kXTC as k increases. The table also presents summary simulated percolation experiment results representing the edge removal steps required to reach a largest connected network component containing half the original topology node population. The percolation results presented in that report demonstrate that k-resiliency builds a network that is more disruption tolerant. Additional details and results can be found in [1], but the table and figure provide a high-level summary of previous analytic experiments. Going forward, the kXTC portion of this report highlights additional detailed network traffic delivery experimentation simulating different resilient levels of topology control.

Table 2—kXTC Average Statistics

	MST	k1	k2	k3	k4	k5	k6
P_{95} transmit power (dBm)	21.61 ± 1.17	23.34 ± 1.42	24.81 ± 1.01	25.73 ± 0.88	26.75 ± 0.95	27.35 ± 0.78	27.87 ± 0.81
Avg. steps before disruption	4.52 ± 2.2	9.00 ± 2.8	33.48 ± 4.04	56.40 ± 3.57	77.96 ± 4.84	99.56 ± 4.95	116.4 ± 3.97

2. SIMULATING k-RESILIENCY AND NETWORK EFFECTIVENESS

To perform network traffic simulation studies of an actual wireless kXTC topology, we initially used the popular network simulator version 3, NS3 [5]. To set up constraints based upon required transmit power, we match NS3 ad hoc wireless communication modem models with a signal-to-noise ratio (SNR) constraint-based model using our Adaptive Networks (*AdaptNet*) software library. The *AdaptNet* software library initially presented in [1] is a Python software toolkit developed by the authors to assist in simulating and analyzing distributed, heterogeneous network topology control problems. *AdaptNet* features include the importing and exporting of wireless network scenarios, various RF propagation models, the calculation of communication path loss and cost matrices for network scenarios, the modeling of heterogenous node characteristics, and the modeling of external interference effects and constraints.

2.1 Topology Cost Constraint Modeling and Tools

For presented studies, we use a set of randomized, static, geospatial node coordinates generated by *AdaptNet*, but other positional models (e.g., group clustering) were examined. To model RF path loss and interference, we leverage Pycraf [6], an open source radio astronomy software toolkit that includes multiple radio propagation models to examine RF interference from external sources. From the scenario models, we develop cost-constrained matrices based upon chosen SNR thresholds for reliable communications between potential network neighbors. As demonstrated in [1], communication link cost matrices may be developed against minimizing external interference thresholds and/or by local transmission threshold constraints in the case of heterogeneous node characteristics.

After defining the cost constraints, we generate a topology and the resultant transmitter profile settings using the specified algorithm approach. Selecting a kXTC network topology calculation results in a set of network neighbors and related transmit power settings within the established cost constraints. To support multicast forwarding in this study, as introduced briefly already, we use the MMTP per neighbor set as each node's transmission power setting. While this is a suboptimal setting for basic unicast-only topology control, this approach supports single-transmission local multicast to established network neighbor links and is an important tactical network design consideration often overlooked in other work.

2.2 Metrics and Random Network Simulations

In the following section, we discuss an initial set of randomized static position experiments performed for both unicast and multicast traffic across a set of generated kXTC topologies. We will later supplement this with mobility and dynamic loss experiments.

To measure network traffic delivery statistics, we adopt a packet delivery ratio metric as shown in Eq. (1). Packet delivery ratio, $PDR_{i,j}$, is defined as the number of unique packets successfully received for flow i at a particular receiver j, $Rx_{i,j}$ divided by the total packets transmitted by a source for that receiver flow, $Tx_{i,j}$. We will present the raw statistical results from simulation trials as a distribution of PDRs using a box and whisker plot. In the multicast case, there are typically multiple receivers for each flow, and poorly located receivers within various topologies may produce sets of low-traffic-delivery performance outliers, yet we include all of these outliers within our raw results. An overall network-wide PDR average, PDR_n, is also calculated as in Eq. (2) and is the average of delivery ratios across all specific receivers for all flows. PDR_n is plotted as a circle within the presented bar and whisker plots of the PDR distributions.

$$PDR_{i,j} = \frac{Rx_{i,j}}{Tx_{i,j}} \tag{1}$$

i is the ith traffic flow at a receiver j

$$PDR_n = \frac{\sum_{i,j} PDR_{i,j}}{\sum_i numRx_i} \tag{2}$$

$numRx_i$: total receivers per $flow_i$

All our experiments were executed using version 3.33 of the NS3 simulator and we leveraged the FlowMonitor functionality to capture source-destination flow statistics such as transmitted packets, received

packets, and loss. However, since the present NS3 FlowMonitor feature supports only unicast traffic models, to support these experiments, we developed a new multicast-capable NS3 FlowMonitor, which is used to measure throughput, hop count, and delay statistics for multicast traffic flows in these studies.

Our initial kXTC network experiments used 50 network scenarios consisting of random geometric node positions for 25 network nodes. Our edge cost constraints in these initial experiments do not involve external interference constraints as we have shown in previous studies [1] and were solely based on transmit power estimates needed to establish reliable network edges in order to study the basic k-resilient relationship to overall traffic transport effectiveness. The presented simulation results used the basic NS3 AdhocWifiMac as the lower layer wireless network model so complex wireless channel contention and packet interference issues are modeled. We present results for a 1 Mbps fixed rate mode of 802.11b direct sequence spread spectrum (DSSS) model with a nominal bit error rate (BER) of 1×10^{-6} and receivers sensitive to signals at –101 dBm. Using *AdaptNet* and this nominal BER, we determine an estimate of minimal transmit power for reliable communications between network nodes. In the actual NS3 physical layer model, a signal-to-interference-plus-noise ratio is used to determine the received packet signal strength against both the receiver noise floor and the sum of other signals received on the current channel [7]. The modeling approach is easily adapted to other ad hoc link layers and constraints, but we chose the existing basic NS3 AdhocWifiMac as an initial basic wireless ad hoc model for evaluation. Within each scenario, we calculate topologies and the required MMTP settings for the least cost minimum spanning tree and kXTC for $k \in \{1, 2, 5, 10\}$. To provide some analytic contrast, we also present a naive common power (CP) scenario using a common transmission power for all nodes based on a reliable communication range of approximately half the diameter of the scenario area. As a note, CP results in a fairly resilient network for random geometric examples, but the naivety of the approach does not guarantee a connected network and we observed disconnected cases for terrain propagation and clustered position scenario models not presented here. For each of these 50 randomized scenarios, we conducted network traffic trials for both unicast and multicast. The next sections discuss and summarize results for each type of traffic experiment. An average summary of characteristic metrics for the 50 scenario topologies is outlined in Table 3.

Table 3—Average Metrics for 50 Randomized Scenarios

	MST	k1	k2	k5	k10	Common power
P_{95} Transmit power (dBm)	18.24 ± 1.32	19.84 ± 1.55	21.59 ± 1.30	24.13 ± 0.89	26.42 ± 0.68	26.15 ± 0.0
Percolation end (edges removed)	4.61 ± 2.18	8.30 ± 2.79	32.40 ± 4.45	97.90 ± 4.81	177.2 ± 3.54	210.1 ± 19.44
Degree	2.049 ± 0.08	2.470 ± 0.23	4.66 ± 0.34	9.84 ± 0.44	15.93 ± 0.35	18.12 ± 1.53
Edges	14.04 ± 1.03	30.88 ± 2.86	58.24 ± 4.25	122.9 ± 5.48	199.1 ± 4.41	226.6 ± 19.18
Diameter	14.04 ± 1.94	9.98 ± 1.64	6.00 ± 0.73	3.68 ± 0.51	2.78 ± 0.42	2.22 ± 0.42

2.3 Simulated Unicast Traffic Experiments and Results

For the unicast traffic experiments, each network traffic trial randomly selected 40% of the node population (10 nodes) to act as traffic source nodes. For each trial, each of the 10 source nodes is paired with a random receiver selection (receiver nodes may be reselected). A total of five randomized traffic trials were conducted over each of the 50 scenarios and source-destination pairs were consistent across trial iterations. Request-to-send/clear-to-send (RTS/CTS) was activated in the NS3 AdhocWifiMac layer as an additional collision avoidance measure for unicast traffic. The default RTS/CTS timeout in the model needed to be increased to allow effective functionality in our longer-range network communication scenarios, especially at higher k values.

Our unicast experiment results shown in Fig. 1 used 1-Kb packet sizes for the traffic flows overtop of a priori shortest path first (SPF) routing. Each bar and whisker plot represents the raw results of all 2,500 PDRs across all 50 random scenarios. Smaller-packet-size trials were conducted as well, but the overall performance trends were similar to these larger-packet trials. Prior to these trials, we validated basic network connectivity with lightly loaded unicast and multicast traffic, and we measured 100% PDR levels for all topologies under study. We then varied flow transmission rates between 30 and 50 Kbps per source to examine PDRs at reasonable levels of network contention and congestion for these scenarios. Results for 30-Kbps flow rates in Fig. 1a demonstrate kXTC is capable of supporting increasingly higher unicast traffic throughput as k resiliency increases. To contrast our results with naively constructed dense topology, we provide PDR distributions for the CP topology, which, as mentioned, employs fixed power control with nodes connecting in a denser fashion but not necessarily as a full clique. As k increases, the average shorter paths resulting between transmitters and receivers helps to reduce contention and increase PDR levels. Absent any adaptive routing or traffic scheduling mechanism, the topology becomes constrained by physical link capacity as transmission rates increase. For example, Fig. 1b shows overall decreased efficiencies for a increased transmission rate of 50 Kbps per network flow but the same general trends in resilience improvements hold.

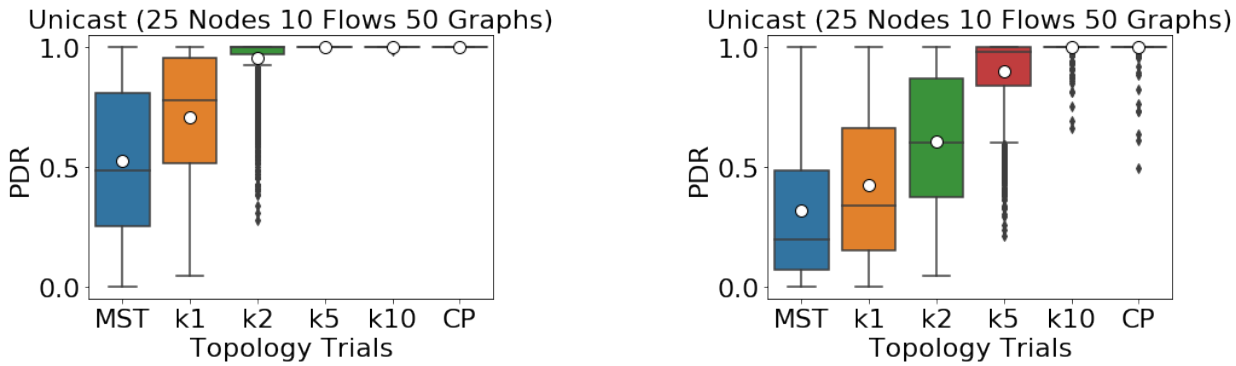

(a) Unicast 30Kbps

(b) Unicast 50Kbps

Fig. 1—Mobile network emulation results: 1-sec intervals

2.4 Simulated Multicast Traffic Experiments and Results

To support multicast forwarding of traffic within the NS3 environment, we developed a basic MANET Simplified Multicast Forwarding (SMF) capability for both classical flooding and essential connected dominating set (ECDS)-type forwarding based upon the existing SMF design specification [8]. Due to the

mesh nature of the forwarding model, multicast packet duplicate forwarding must be avoided at each node through a packet duplicate detection method as described in the SMF specification. Some additional NS3 modifications were required to achieve the correct packet duplicate detection functionality needed.

Figure 2 presents graphical summaries for a set of multicast cases studied. While we executed many different traffic experiments, we present results from a traffic model of 10 multicast flows of 20 Kbps with all nodes acting as multicast receivers in the experiment. As in the unicast case, we measure and use PDR for each receiver and across all packet flows as the primary performance metric for the least cost MST, $k \in \{1, 2, 5, 10\}$ kXTC, and CP topologies.

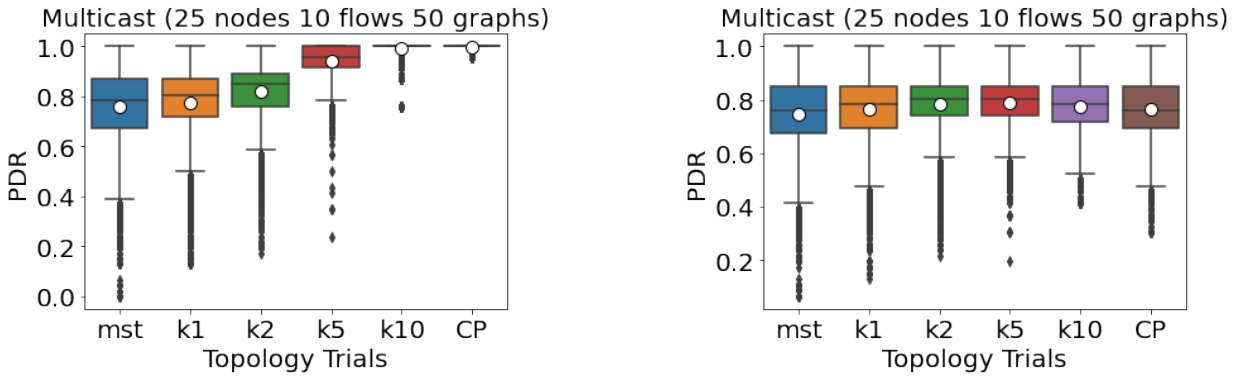

(a) ECDS Forwarding

(b) Classical Flooding

Fig. 2—Mobile network emulation results: 1-sec intervals

Our first observation from Fig. 2a is that MST and XTC ($k = 1$) demonstrate similar results for the cases studied. This is expected, as XTC in its basic $k = 1$ form is close to MST in terms of network diameter and density and results in similar overall network performance and transmission power settings.

Our second observation related to Fig. 2a is that as k increases, we observe marked improvements in overall packet delivery ratios when using the ECDS multicast approach. At this data rate, contention level improvements at $k = 2$ are less significant, only reducing some of the poorly performing receivers and outliers. We observe that at $k = 5$, the PDR dramatically improves alongside the topological redundancy, but for this scenario, the average transmission power cost also increases significantly as seen in Table 3.

There are rather complex trade-offs in this case, since the NS3 AdhocWifiMac layer adopted is susceptible to hidden terminals and contention and in the multicast model case lacks the contention suppression of the unicast RTS/CTS mechanism. The longer network forwarding paths increase both contention and communications events required for delivering group data across the network. The use of an ECDS variant of the forwarding process improves PDR as networks become more k-resilient but has little effect in the MST case, as there is minimal topological redundancy. Again, for higher values of k (e.g., $k = 5$) there appear to be significant PDR and resiliency improvements, but there is also an increasing transmission power cost penalty for the wireless architecture models used.

The classical flooding multicast results in Fig. 2b demonstrate quite a different effect from the ECDS results, as PDR improves slightly for moderate k increases and then decreases slightly as network topologies reach higher densities. In these test cases, even though the network diameter decreases as k increases, the

inefficient forwarding of classical flooding causes increased traffic contention and congestion due to excessive redundant retransmissions. We realize these results are not independent of network medium access control (MAC) layer characteristics under study and will discuss opportunities for further network optimizations in future work, but the general trend demonstrates the importance of managing traffic forwarding efficiently even when deploying increasingly resilient topologies.

3. DYNAMIC AND MOBILE EXPERIMENT RESULTS

In this section, we examine the efficacy of a k-resilient topology control in terms of supporting various forms of network traffic and MANET routing under network dynamics, including both mobility and temporal link loss modeling within distributed wireless networks. Work presented in earlier sections was limited to performance and resilience of unicast and multicast traffic loads in randomized static network topology models. Here, we present and discuss additional dynamic performance experiments, including graph-based analytic models, simulation in network simulator version 3 (ns3), and emulation using the Extensible Mobile Ad hoc Network Emulator (EMANE). Future Navy collaborative wireless tactical networks may often consist of moderately sized ad hoc networks; we therefore chose to examine mobile network consisting of 30 nodes for this study, although kXTC is scalable in operations. We also chose to examine communication graph models from MST (minimum resilience) up through a high level of k-resilience (i.e., k=10).

3.1 Simulated Network Fading With Topology Control

To assess the resilience to failures of various topology control settings, we conducted a link failure study in which we subjected each link independently to an additive Gaussian fading parameter at an interval we have termed the fading interval. When conducting a fading simulation, we initially model the loss without a fading parameter to determine the initial topology and connections. Then, at the fading interval, we inject additional loss onto each link augmenting the original network matrix of losses into a new fading matrix according to Eq. (3).

$$\begin{aligned} \text{fadingMatrix}_{i,j} &= \text{lossMatrix}_{i,j} + \mathcal{N}(\mu, \sigma^2) \\ &\text{where} \\ \mu &= 0 \\ \sigma &= \text{fadingFactor} \\ \text{fadingFactor} &\in [0, \text{inf}) \end{aligned} \tag{3}$$

The Network Simulator 3 (NS3) network modeling environment was used to conduct a series of link fading studies. The NS3 scenario parameters used for this initial study include: free space loss propagation, the AdhocWifiMac MAC layer, and a 1 Mbps basic link rate configuration. After calculating the updated fadingMatrix that includes the fading perturbation at the time of a topology update, we update the topology constraints (e.g., routing, transmit power, neighborhood). In order to study the k-resilience with different fading rates, we examine both 10-second and 1-second fading intervals. This setup was conducted for five tests each of random starting position of network nodes for fading factor values 0, 2, 5, 10, 15, and 20. To measure the network traffic delivery ratio, we use the packet delivery ratio (PDR) defined in Eq. (1). Figure 3 presents some summary results of our NS3 simulation trials with various types of PDR traffic measures

for both unicast and multicast. We do not present the classical flooding (CF) multicast cases here, since k-resilience provides less value due to the built-in redundancy of CF duplicate network forwarding paths. We remind the reader that this redundancy comes at a cost and that CF suffers from poor overall performance due to the increased congestion and contention caused in the network.

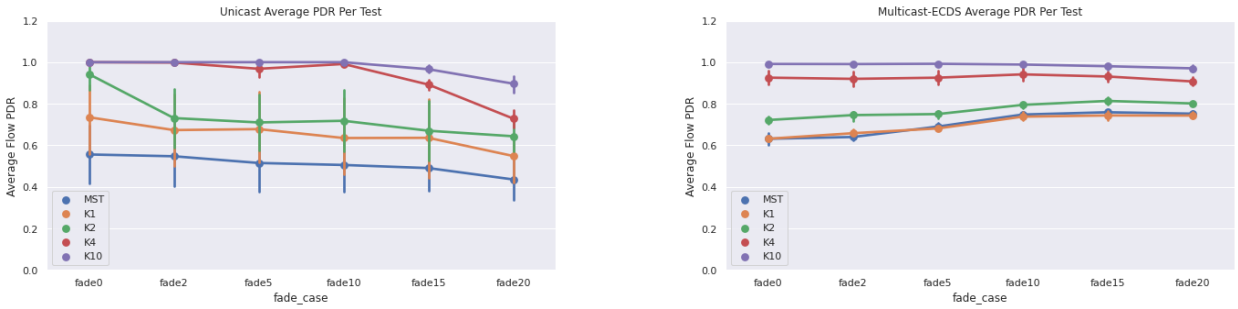

(a) Unicast with fading

(b) ECDS Multicast with fading

Fig. 3—NS3 simulated fading scenarios

Figure 3a presents results at various levels of fading averaged across a series of unicast traffic flow tests in ns3. We observe that, as might have been expected, higher levels of k-resilience provide improved performance against fading channel effects within the network for unicast traffic. In contrast to multicast, unicast forwarding using single paths is more subjected to random disruption caused by independent link fading conditions.

Figure 3b presents results at various levels of fading averaged across a series of multicast traffic flow tests using ECDS backbones as a forwarding mechanism within the network. We observe that k-resilience provides value in these cases similar to the unicast cases, but that there are also some interesting observations of slightly improving performance as fading gets worse. Since the fading is modeled as an independent and identically distributed (i.i.d.) process, this can be partly explained as an outcome of reduced contention and receiver interference for some receiver paths, since receiver interference noise is additive and especially relevant in sparser network with more hidden terminals.

3.2 Network Mobility Models With k-Resilience

The mobility scenarios we applied in this study were RandomWaypoint scenarios generated by the well-known *bonnmotion* scenario generation tool. For each topology class, we examined 10 randomized trials of 300 time steps, and from each bonnmotion mobility scenario topology update period, we calculated a cost constrained topology and a set maximum transmission power profiles. We plot rate of change and resulting MMTP characteristics for the mobility scenarios in Fig. 4. Each topology type has different neighbor update rate statistics due to the different densities, and Fig. 4a plots the average rate of change during a topology update for each topology type and mobility scenario used in this study. While the kXTC cost constraints can include non-distance-correlated costs including terrain propagation and other effects, the results presented here are based upon free space loss and a 1-Mbps wireless waveform model. Figure 4b plots the constrained maximum transmission costs resulting for each topology type across all mobility scenarios used in this study.

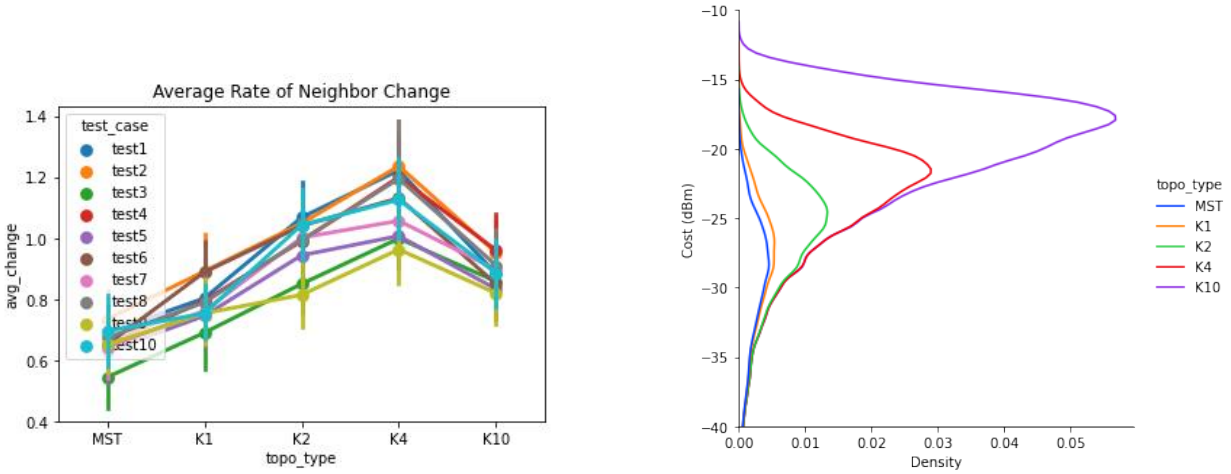

(a) Rate of change

(b) MMTP cost distributions

Fig. 4—Mobile scenarios

3.3 Emulated Mobile Network With Topology Control

In this section, we measure network traffic delivery ratios in a series of random mobility experiments with 1- and 10-second-interval mobility update rates and k-resilient topology maintenance updates occurring at 10-second intervals. In practice, network-wide topology maintenance updates will likely occur at a slower update period than link dynamics caused by mobility or other temporal effects, so we are interested in examining the ability of the k-resilient topology to not only update and track the mobility, but to provide increased operational resilience during periods between topology updates. To measure performance, we use the same PDR metric explained in Section 2. EMANE with the 802.11abg model is used here, with unicast and broadcast base link rates set to 1 Mbps. In unicast scenarios, 10 traffic flows of 30 Kbps are sourced from random source nodes to random destination nodes. For multicast scenarios, the traffic model is 10 random nodes sourcing traffic flows of 20 Kbps to a multicast address that is received by all nodes in the network.

Figure 5 presents unicast and multicast results for emulated mobility scenarios in which both mobility and topology updates occur at 10-second intervals. Figure 5a shows the unicast average PDR per flow across a variety of topology densities with mobility and kXTC topologies. In addition to faster rate dynamics in the environment, network routing protocols themselves may suffer from dynamic link estimation errors and stale information. So to examine real-time routing vs. optimal global routing performance, we plot PDR performance using a priori Dijkstra shortest-path-first (SPF) routes (labeled "unicast" in the graph), as well as Optimized Link State Routing (OLSR) [9] with both default specification timers and faster timers (0.5-second hellos, with other timers scaled appropriately). As shown in previous work with static topology experiments, average PDR increases with increasing topology resilience (i.e., higher k). OLSR with faster timers also improves PDR performance across all topology cases when compared to OLSR with default timers and manages to approach the performance of the more idealized a priori calculated route cases.

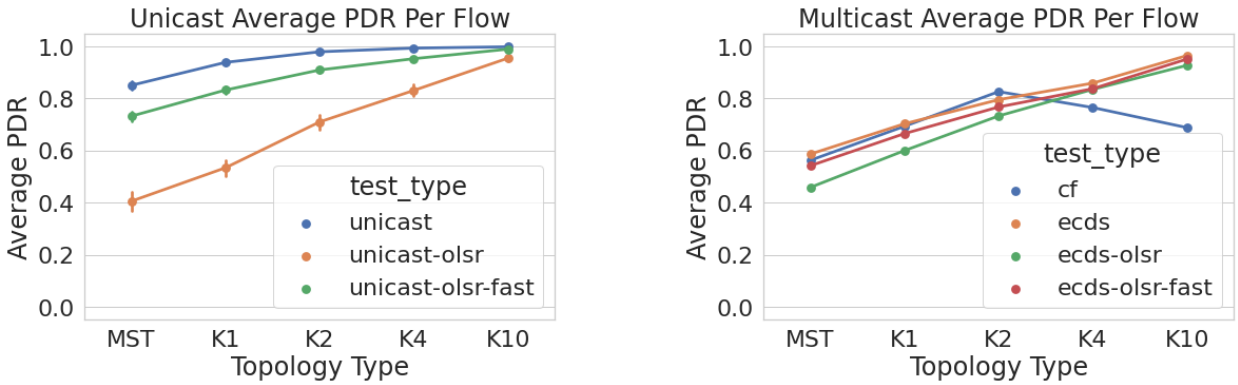

(a) Unicast

(b) Multicast

Fig. 5—Mobile network emulation results: 10-second intervals

Figure 5b similarly shows multicast average PDR per flow across a variety of topology densities using classical flooding (CF), an a priori-calculated ECDS relay set, and online ECDS relay sets that are dynamically determined at runtime using OLSR with default and faster timers. CF results show increases in PDR up until $k = 2$, then PDR drops due to the increased congestion/contention caused by using classical flooding with higher-density networks. For ECDS, higher densities provide increasing PDR due to fewer necessary transmissions. A priori-calculated ECDS as well as the ECDS relay sets calculated by OLSR provide similar results, with a priori ECDS maintaining a slight advantage over more realistic dynamic ECDS-based routing calculations. As expected and similar to unicast results, ECDS calculated by OLSR with faster timers maintains an advantage over the slower timers, particularly at lower k, but the difference is not as significant as that seen with unicast results. This is likely due to continued support of additional redundant paths by ECDS multipath forwarding in the network, whereas precalculated single-path SPF unicast forwarding is more fragile to any topology perturbations.

When deploying topology control algorithms, the update rate for new topologies is likely to change at a slower pace than mobility changes, so we reran the previous EMANE mobility experiments with faster mobility rates while keeping the topology update rate fixed at 10 seconds. Figure 6 presents unicast and multicast results for emulated mobility scenarios in which mobility updates occur at faster 1-second intervals and topology control update rates remain at 10-second intervals.

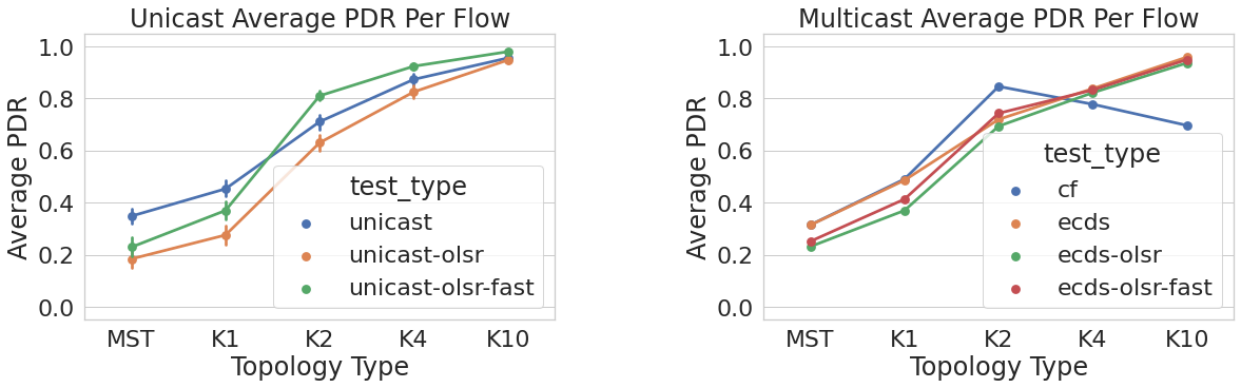

(a) Unicast

(b) Multicast

Fig. 6—Mobile network emulation results: 1-second intervals

Figure 6a shows the unicast average PDR per flow across a variety of topology densities at faster mobility rates. Due to the faster update rates, additional link failures will occur due to increased mobility changes before a newer topology update can adjust. We observe that for low resiliency topologies (e.g., MST, $k1$) PDR performance suffers significantly, since the topologies constructed are more fragile and have a higher probability of becoming fragmented during periods of additional mobility. We also observe the general trend that higher resilience protects against some of this temporal disruption, since additional network link redundancy exists and allows routing protocols to discover and adapt to these changes. Of particular interest is that k levels as low as 2 provide significant performance improvement jumps compared to more *MMTP-optimal* MST and k=1 settings. This is valuable engineering insight into the practical use of topology control combined with adjustable resilience.

It should also be noted that using a priori shortest-path calculations ("unicast" in Fig. 6a) no longer represent an idealized case, as those routes are only updated every 10 seconds when the topology updates, so they may become broken by mobility updates, whereas runtime-calculated routing updates are able to adjust to dynamics and find alternative routes. This is why OLSR with the faster update rate outperforms the a priori calculation at higher k — OLSR in that case is updating its topology view and routing paths more often than every 10 seconds. At lower k, we suspect this effect is absent because mobility updates are more likely to cause network fragmentation where there are no alternative routes available.

Figure 6b shows the multicast average PDR for the same faster mobility trials, and we observe similar trends with lower-resiliency topologies suffering more during periods of additional disruption. As before, CF performs poorly as topologies become more dense due to additional transmission power and increased contention and congestion conditions. We see similar behavior as in the unicast case, where ECDS calculated using an OLSR protocol with faster timers outperforms the a priori ECDS calculation mode at higher densities only, though the difference is much less significant when compared to unicast results.

4. NETWORK BACKBONE FORMATION WITH EXTERNAL CONSTRAINTS

4.1 Power Control and Cumulative Power Emission

In [2], we focused on the problem of constructing the largest connected component of an ad hoc network while ensuring that the cumulative power from the network component remains below an interference or

sensitivity threshold at an external node. The link costs that contribute to the cumulative power were based on a power control scheme that chose the minimum power required to close the link. We have applied this model to a related problem of network topology management, namely forming a network backbone as a connected dominating set (CDS) with similar external node considerations.

The motivation for studying the network backbone or CDS problem lies in the potential for incorporating additional degrees of freedom in limiting interference power at an external node, such as additional frequency bands, beamforming or directionality gain, or other waveform characteristics. Organizing the network into a backbone network and connected leaf nodes results in a two-layer, hierarchical structure that can enhance network capacity when exploiting the extra degrees of freedom.

As the density of wireless networked devices increases for military and commercial applications, power control becomes a critical function for the formation of ad hoc networks. Through power control, networks can limit in-network interference to increase network throughput, limit interference to nodes or devices external to the network of interest for coexistence, and reduce power and transmission range to extend network lifetime. While many studies have focused on the interference from individual nodes, it is well known that interference is more accurately modeled as the cumulative power from all active transmissions, known as the physical interference model [10], which is considered here.

4.2 Minimum Power Connected Dominating Set Problem (MPCDS)

While the LCT problem focused on staying within a given threshold on the cumulative power experienced by an external node, we now consider an inverted version of the problem in which we minimize the cumulative power experienced to connect an ad hoc network. We are interested in building a *backbone* (as a *connected dominating set*) within the network such that the resulting network minimizes interference to the external node. As in [2], we focus on centralized approaches with global knowledge of the problem, which will provide a bound on the achievable utility or cost. Developing distributed, localized algorithms will be the focus of future research.

4.2.1 Network Model

We study a wireless network consisting of nodes placed in a square deployment area. There is a receiver threshold ϕ that must be met to close a link between two nodes in the network. The transmit power required to successfully transmit from node u to node v is $P_T(u,v) = \phi + pathloss(u,v)$ (dB). There is an external node x that is not part of the network, and we would like to limit the amount of power emitted from the network that is incident on the node. The received power at the external node for a transmission from node u to node v in the network is given by $P'_R(u,v,x) = P_T(u,v) - pathloss(u,x)$ (dB). The sum of the powers in both directions, which will be assigned as the cost of the link, is given by $P_R(l,x) = P'_R(u,v,x) + P'_R(v,u,x)$, where $l = (u,v)$. The total power received from some set of active links L in the network is given by $P_R^{tot}(L,x) = \sum_{l \in L} P_R(l,x)$. We would like to minimize the total received power required for a particular network topology formation.

We also include a network activity level parameter $\alpha \in (0,1]$, since typically not all links will be active in both directions 100% of the time. This parameter can be either viewed as the highest level (upper bound) of network activity or some average level, depending on how conservative the network operator needs to be or how sensitive the external node is. In either case, the total received power is given by $\alpha P_R^{tot}(L,x)$.

4.2.2 MPCDS Graph Model

The networking problem we consider is to construct a backbone network with minimum cost by choosing a connected dominating set (CDS) of the network graph. A CDS is defined as a connected set of nodes in which all nodes in the graph are either in the CDS or have an edge connecting it to the CDS. The initial wireless network graph is given as a complete graph $G(V, E)$ with nodes $V = \{1, 2, \ldots, n\}$. Undirected edges $(u, v) \in E$ that are used to connect the CDS incur a cost, and the nodes that are not part of the CDS (leaf nodes) incur a flat cost $\zeta\bar{w}$. This flat cost models a two-layer hierarchical network structure separating backbone and leaf nodes, where the cost approximates the reduced power required for the leaf nodes to communicate with the backbone due to some directionality gain or out of band communication. We vary the parameter ζ, which is the proportion of the average edge cost, $\bar{w} = \sum_{e \in E} w(e)/|E|$, at which the flat cost is set. Using $\bar{w}$ normalizes the flat cost to the specific network characteristics. We would like to find the set of nodes that forms a connected dominating set (CDS) such that the sum of the cost of the edges required to connect the CDS (the minimum spanning tree of the CDS) and the flat cost of the leaf nodes is minimized.

$$\begin{aligned} \min_{G' \subset G} \quad & \textstyle\sum_{e \in E(G')} \alpha w(e) + |N(G) \setminus N(G')|\zeta\bar{w} \\ \text{s.t.} \quad & \text{Nodes in } G' \text{ form a CDS,} \\ & \text{edges in } G' \text{ form its MST,} \end{aligned} \tag{4}$$

where $E(G)$ is the set of edges in graph G, $N(G)$ is the set of nodes in set G, and $N(G) \setminus N(G')$ is the set of nodes in G that are not in G'. We call this the minimum power CDS (MPCDS) problem.

4.3 MPCDS Mixed Integer Linear Program Solution

In some integer programming formulations for minimum spanning trees, subtour elimination or cutset approaches are used in which a constraint is defined for each subset of vertices. In this case, the problem is exponential in the number of constraints and cannot practically be programmed into a software-based solver. For a formulation that is polynomial in the number of constraints and variables, we adopt the approach from [11], which is a mixed integer linear program (MILP). We used a very similar approach for the LCT problem in [2]. We construct a new directed graph G_{MPCDS} by augmenting the original graph G with two nodes $n + 1$ and $n + 2$, converting the undirected edges $e = (i, j) \in E$ into pairs of directed edges (i, j) and (j, i), each with edge cost $w_{ij} = w_{ji} = w(e)$, and adding directed edges from $n + 1$ and $n + 2$ to every node in V and $(n + 1, n + 2)$. We assign cost $\zeta\phi$ to edges from $n + 1$ to the other nodes in V ($w_{n+1,j} = \zeta\phi, \forall j \in V$), and the remaining edges (connected to $n + 2$) have zero cost.

The MILP is formulated in similar fashion to the LCT problem, with a different objective function and slight alteration of the constraints. The decision variables are x_i and y_{ij} for whether node i and edge (i, j) are included in the CDS, and the objective is to minimize the cost of edges chosen: $\sum_{(i,j) \in A} \alpha w_{ij} y_{ij}$. The idea is to build a tree with G_{MPCDS} such that nodes in the CDS are connected to node $n + 2$ via a root node, and the nodes not included in the component are connected directly to node $n + 1$. The problem is formulated as

follows:

$$\text{maximize} \quad \sum_{(i,j)\in A} \alpha w_{ij} y_{ij} \tag{5}$$

$$\text{subject to} \quad \sum_{j\in V} b_{ij} x_j \geq 1 \qquad \forall i \in V \tag{6}$$

$$\sum_{i\in V} y_{n+2,i} = 1 \tag{7}$$

$$\sum_{i:(i,j)\in A} y_{ij} = 1 \qquad \forall j \in V \tag{8}$$

$$y_{n+1,i} + y_{i,j} \leq 1 \qquad \forall (i,j) \in A \setminus E' \tag{9}$$

$$(n+1)y_{ij} + u_i - u_j + (n-1)y_{ij} \leq n \qquad \forall (i,j) \in A \setminus E' \tag{10}$$

$$(n+1)y_{ij} + u_i - u_j \leq n \qquad \forall (i,j) \in E' \tag{11}$$

$$y_{n+1,n+2} = 1 \tag{12}$$

$$u_{n+1} = 0 \tag{13}$$

$$1 \leq u_i \leq n+1 \qquad i \in V \cup n+2 \tag{14}$$

$$x_i + y_{n+1,i} = 1 \qquad \forall i \in V \tag{15}$$

$$x_i, y_{ij} \in \{0,1\} \qquad \forall i \in V, (i,j) \in A, \tag{16}$$

where E' is the set of directed edges connected to $n+1$ or $n+2$ and A is the set of all directed edges (two for each edge in E, and E'). The variables x_i and y_{ij} are the decision variables for whether node i and edge (i,j) are included in the MPCDS's minimum spanning tree. The variables u_i are used to eliminate subtours. Constraint Eq. (6) ensures that the chosen network is a dominating set where b_{ij} is the (i,j)th element of the adjacency matrix of the original graph G, Eq. (7) is for the edge connecting $n+2$ to the root of the MPCDS tree, Eq. (8) is to ensure that all of the original nodes have exactly one neighbor, Eq. (9) ensures that if an original node is connected to another original node then it is not connected to $n+1$, Eqs. (10) and (11) are the Miller-Tucker-Zemlin constraints [12] to ensure there are no subtours, Eq. (12) connects nodes $n+1$ and $n+2$, Eqs. (13) and (14) are the valid range of values for the variables u_i, Eq. (15) indicates that a node is either in the tree connected to $n+2$ or directly connected to $n+1$ and not part of the MPCDS, and Eq. (16) defines the x_i and y_{ij} as binary decision variables. In our simulations, we solve this problem computationally using CVXPY [13], a Python package for convex optimization, and we used the Cbc solver [14], which is an open-source solver that uses a branch-and-cut approach for mixed integer linear programs.

4.4 MPCDS Simulation Results

To validate our MILP formulation for the minimum power CDS (MPCDS) problem, we conduct a Monte Carlo simulation study for different network sizes, node densities, and other network characteristics. The cost model measures the interference power at the external node using free space propagation. Although these costs are based on simple geometric models, the MILP formulation can accept arbitrary cost models, including precomputing complex real-world propagation models.

4.4.1 Eight-Node Example

We first simulate the MPCDS algorithm for a single network. We set the receiver threshold ϕ to 5×10^{-10} Watts, and the N nodes are uniformly randomly deployed in a square region with side equal to $10\sqrt{N}$ meters.

In addition to the mixed integer linear program (MILP) approach, we also implement a brute force (BF) approach, which is an exhaustive search of all combinations of nodes for the CDS. Each algorithm (MILP and BF) runs for a maximum time of 1,000 seconds before returning the best solution found.

An example of an $N = 8$ node network is shown in Fig. 7 with the external node placed at a distance of $10d\sqrt{N}$ meters 45 degrees from the center of the original deployment area, with $d = 1$. The network activity level α is 1. We see that the brute force (BF) approach and the mixed integer linear program (MILP) approach both find a CDS of size 3 and cost 1.569×10^{-9}.

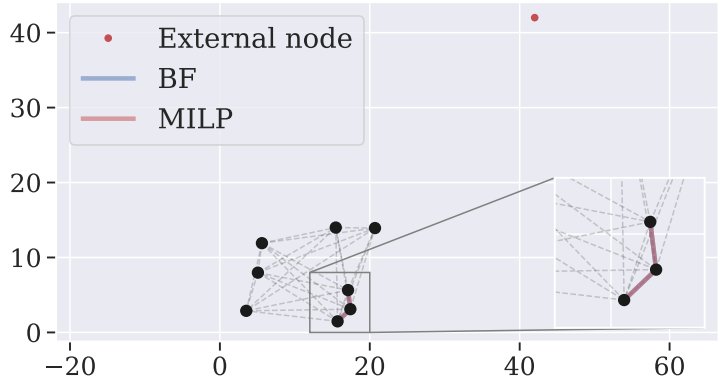

Fig. 7—Eight-node MPCDS example, $\zeta = 0.5$, $d = 1$, $\alpha = 1$

4.4.2 Increasing Network Size, Fixed Node Density

We have simulated the MPCDS algorithms for different network sizes. For each case of network size, we ran 50 instances of randomly placed nodes, and if the average execution time exceeded 300 seconds, we stopped increasing the network size. For each instance of node placement, each algorithm runs for a maximum time of 1,000 seconds before returning the best solution found. This is to ensure that the simulations run in a reasonable amount of time. We first focus on the case of constant node density, where each side of the deployment area is scaled by $10\sqrt{N}$, and the cost constraint C is fixed at 5×10^{-10}. The external node is placed 45 degrees from the original deployment area, and the distance between the center of the network deployment area and external node is $10d\sqrt{2N}$.

The average execution time for the MPCDS problem is shown on a log scale in Fig. 8a. The execution time for the BF is comparable to the MILP for the network sizes shown, but it appears that the MILP execution time grows at a slower rate. The average minimum cost and CDS size are given in Fig. 8b for $\zeta = 0.1$ and Fig. 8c for $\zeta = 0.5$ (these values of ζ were shown to be representative of a wide range of edge costs). As expected, the average cost and the CDS size are larger when the leaf cost is higher ($\zeta = 0.5$). For $\zeta = 0.1$, the CDS size is larger for $d = 5$ than $d = 0$, since it is less costly to join the CDS with the farther external node. For $\zeta = 0.5$, the full network is in the CDS.

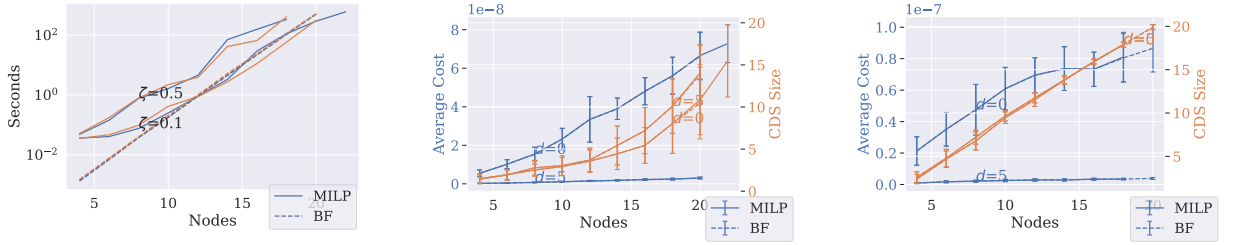

(a) Execution time vs. network size

(b) CDS cost and size vs. network size, $\zeta = 0.1$

(c) CDS cost and size vs. network size, $\zeta = 0.5$

Fig. 8—MPCDS for increasing network size, fixed node density, $\alpha = 1$

4.4.3 *Increasing Network Size, Increasing Node Density*

The next simulations also look at increasing the number of nodes, but the side of the deployment area is kept constant at 10 meters, so the node density increases with network size. The external node is again placed 45 degrees from the original deployment area, but now the distance between the center of the network deployment area and external node is $10d\sqrt{2}$. The average minimum cost and CDS size are given in Fig. 9a for $\zeta = 0.1$ and Figure 9b for $\zeta = 0.5$. Compared to the fixed density case, the average cost is smaller, since the nodes are closer together and the edge costs are smaller. Since the leaf costs are normalized to the average link cost, there is no discernible difference between the CDS sizes for fixed and for increasing node density.

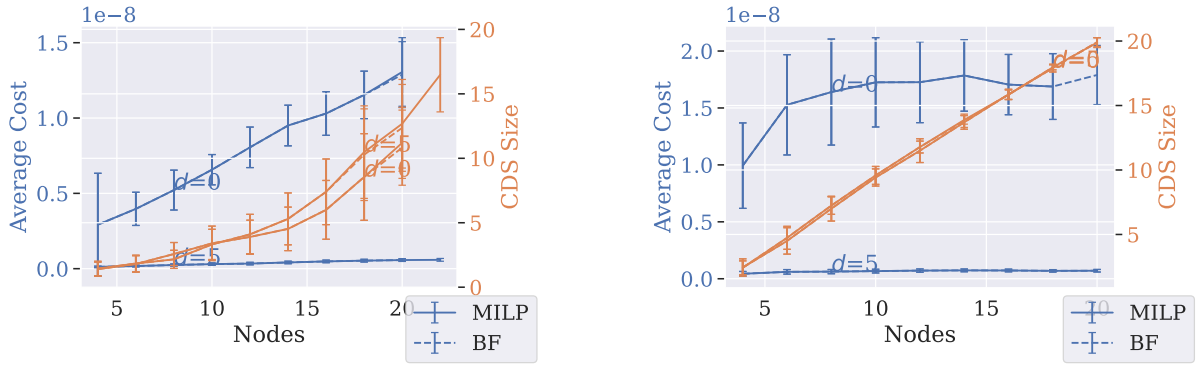

(a) CDS cost and size vs. network size, $\zeta = 0.1$

(b) CDS cost and size vs. network size, $\zeta = 0.5$

Fig. 9—LCT and MPCDS for increasing network size, increasing node density, $\alpha = 1$

4.4.4 *Increasing Network Activity*

Next, we simulate for networks of 14 nodes with different external network activity levels α. We omit the brute force approach due to the long execution time for 14 nodes. We simulate a lower-node-density case (side of deployment area equals $10\sqrt{N}$, external node distance is $10d\sqrt{2N}$) and a higher-node-density case (side equals 10, external node distance is $10d\sqrt{2}$) for $d = 5$. The results for CDS cost are shown in Fig. 10a for $\zeta = 0.1$ and Fig. 10b for $\zeta = 0.5$. The average cost increases with activity level since it is directly proportional. The CDS size is independent of the activity level, since it just scales the objective function and does not affect the rest of the problem.

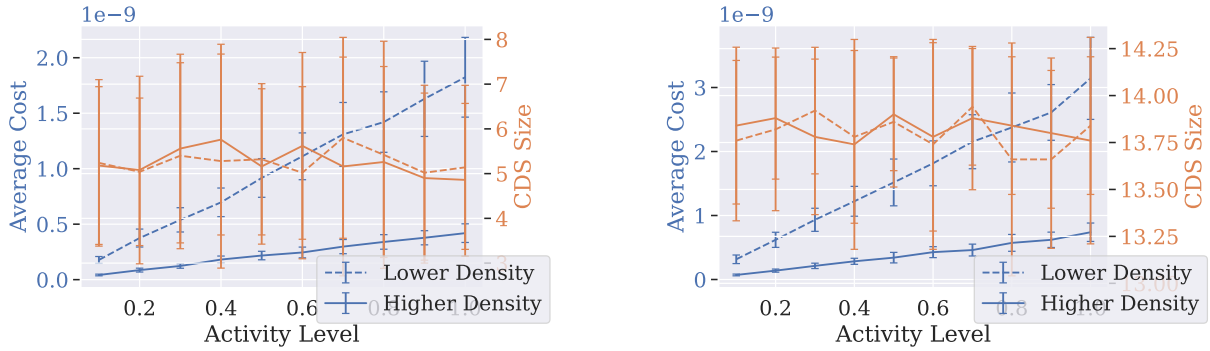

(a) CDS cost and size vs. network activity, $\zeta = 0.1$

(b) CDS cost and size vs. network activity, $\zeta = 0.5$

Fig. 10—MPCDS for increasing network activity, $N = 14$, $d = 5$

4.4.5 Increasing External Node Distance

To understand the impact of the distance of the external node on the network connectivity and power emitted, we fix the network size at 14 nodes and simulate for different external node distances d. We consider both lower-density (side equals $10\sqrt{N}$) and higher-density cases (side equals 10). We ran this simulation for $\zeta = 0.1, 0.5$, and we see in Figs. 11a and 11b the cost decreases with d, since the external node is getting farther away from the network. We note that the CDS size does not seem to depend on the external node distance, since the edge costs relative to one another do not change much as the external node gets farther away, and the leaf node cost is normalized to the edge costs.

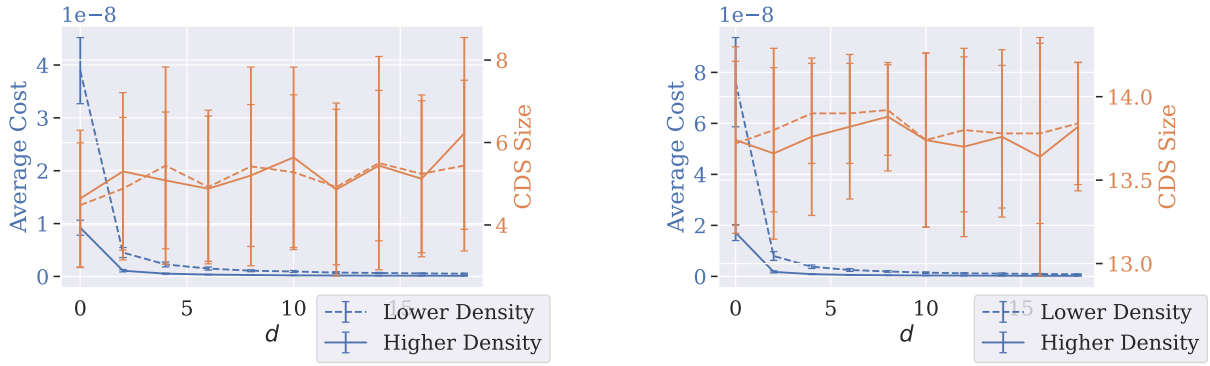

(a) CDS cost and size vs. external node distance, $\zeta = 0.1$

(b) CDS cost and size vs. external node distance, $\zeta = 0.5$

Fig. 11—MPCDS for increasing external node distance, $N = 14$, $\alpha = 1$

4.5 Simulation Summary

As a companion to our work in [2], we studied another problem for ad hoc network formation under sum power interference constraints: to form a backbone network that minimizes the sum power incident on an external node, which we formulated as the minimum power connected dominating set (MPCDS) problem. We

formulated the mixed-integer linear program for each problem that is polynomial in the number of constraints and variables, which can be solved computationally. Simulation results characterize their performance, which is better for higher node density or lower network activity.

5. ENERGY HEATMAPS FROM THROUGHPUT OPTIMIZATION

In addition to the topology control and optimization, we have begun investigating throughput optimization with external constraints. Specifically, we apply a spatial reuse technique to schedule links simultaneously such that an SINR threshold is satisfied, subject to a constraint on the total energy absorbed by the external node over a scheduling period. The routing and scheduling are optimized for some notion of fair throughput for traffic flows between all of the nodes and a gateway node, which is formulated as a linear program. Since the number of potential sets of links and routes that can be utilized in the schedule is exponential in the number of links, we apply a column generation approach to iteratively solve the linear program for reduced solution spaces. The approach is based on the work in [15].

Some preliminary results are included in this report in Fig. 12, where we have plotted the average energy heatmap results from a Monte Carlo simulation for randomly placed networks of 10 nodes, where the average is over 50 random node placements for which the fair throughput routes and schedules were optimized. Simulation parameters are given in Table 4. The figures color code the energy absorbed at each point in the map due to the transmit powers and durations resulting from the constrained optimization over a single period, with the corresponding energy values in dB. We observe that as the external node location (marked by the "x") moves farther away from the main network, the energy put out by the network increases, and the average network throughput increases from 185.40 Kb/s to 188.79 Kb/s to 191.99 Kb/s. These preliminary results will be part of a larger study to be published in the near future.

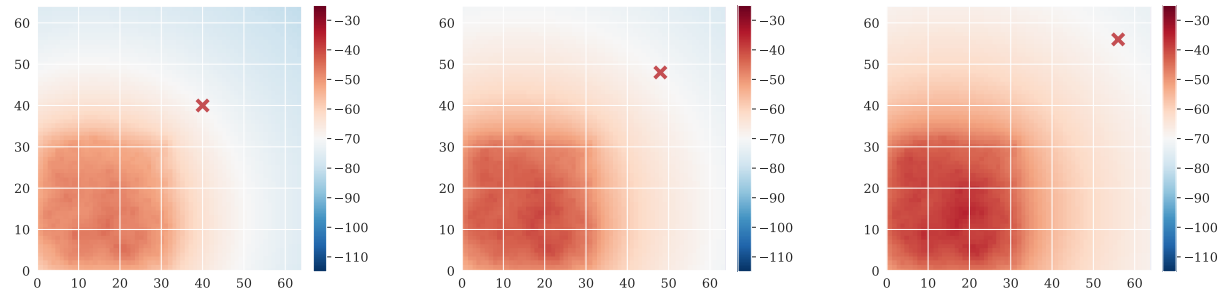

(a) Heatmap (in dB), $d = 0.75$ (b) Heatmap (in dB), $d = 1$ (c) Heatmap (in dB), $d = 1.25$

Fig. 12—Heatmaps for increasing external node ("x") distance d, interference threshold $\eta = -70$ dB

Table 4—Simulation Parameters

Nodes	10
Deployment area	30×30 m
Rates	{164, 328.12, 393.75, 492.18, 590.625} Kb/s
SINR requirements	{1, 10, 11.4, 11.8, 13.8} dB
Maximum transmit power	30 dBm
Noise power	-13 dBm
Path loss exponent	3.6
Near-field crossover distance	1 m

6. FUTURE WORK

The research discussed in this report has developed and explored some new approaches to wireless network topology control. As presented in Section 1.2, the work has gone beyond past research by focusing in more detail on the following challenges: topology resilience, traffic effectiveness, heterogeneity, generic cost constraints, and dynamic emulation modeling. This initial work has focused largely on single-channel wireless operation and basic modeling of ad hoc CSMA/CA MAC layers. We plan on exploring additional areas in future work that we believe will have significant additional impacts on both resilience and operational effectiveness. The consideration of network directivity, additional MAC layer designs, and multichannel wireless network capabilities can reduce some of the transmission cost of building additional resilient network structures as studied in this report and also will likely improve network traffic delivery ratios achievable at lower k levels of network resilience. We have demonstrated that the ability to improve network traffic delivery ratios at low to moderate levels of k-resilience is an important issue for wireless tactical networks, which need to balance effectiveness against operational dynamics and risk. Therefore, future studies are planned to examine network directivity and additional heterogeneous network architecture models using similar cost-constrained topology control and adaptation mechanisms.

In addition, we plan to further explore the research and designs begun here on tiered operation of topology control using CDS backbone construction with an external node constraint. One area to explore is enhancing the flat cost for leaf nodes to model multichannel architectures or directionality gain, and find the minimum received power at an external node. We are also interested in other heterogeneity in the network, including other modes of communication such as free space optical links, or having nodes with uneven RF capabilities. The external constraint is another area that needs further study, including multiple external nodes or uncertainty in node locations. Finally, we would like to incorporate the throughput optimization after creating these ad hoc network structures, such as the largest constrained tree or the CDS-based network, and to compare with throughput optimal scheduling without such network structures.

7. CONCLUSIONS

In summary, this report extends earlier analytic work in adjustable k-resilient wireless network topology control [1] by evaluating unicast and multicast traffic delivery ratios across a series of simulated k-resilient topology experiments using the NS3 network simulator and emulated network experiments using EMANE capability. We introduced NS3 simulation extensions to support multicast traffic evaluations and discussed the *AdaptNet* library toolkit, which provides a variety of capabilities for constraint-based topology control, such as modeling complex propagation and analyzing spectral emissions caused by the network. *AdaptNet* was used

in conjunction with the NS3 simulations and EMANE emulations presented to establish the cost-constrained k-resilient topology networks using the developed kXTC algorithm.

We conclude from our initial randomized network simulations that even moderate levels of k (e.g., 2–5) provide significant communication delivery improvements while constructing increased network edge connectivity under a set of given cost constraints. Further dynamic studies presented in this report include both link fading conditions and mobility and further demonstrate that moderate levels of k-resilience provide increased traffic delivery performance improvement. Moderate levels of k-resilience also help to alleviate the disruptions caused by network dynamics, such as mobility, that often occur on shorter timescales than topology update periods.

This report also follows up work on constructing the largest tree in an ad hoc wireless network subject to external node constraints [2], where here we construct a network backbone as a connected dominating set to minimize the cumulative transmit power absorbed at an external location. The mixed-integer linear program formulation enabled us to use a computational solver and perform a Monte Carlo simulation study, which provided an extensive characterization of the performance of the average cost under a wide range of network parameter settings. We also presented some preliminary findings on our ongoing throughput optimization effort, specifically, some network energy heatmaps resulting from Monte Carlo simulation of random node placement. The results demonstrate throughput improvement and a decreased adaptive power footprint as the external target location moves closer to the network.

REFERENCES

1. J. Macker, C. Bowers, S. Kompella, and C. Kam, "Wireless Network Topology Control: Supporting Link Cost Constraints and Resiliency," NRL/FR/5522- -20-10,404, Naval Research Laboratory, https://apps.dtic.mil/sti/pdfs/AD1116830.pdf, Dec 3, 2020.

2. C. K. Kam, S. Kompella, C. Z. Bowers, and J. P. Macker, "Network Sum Power Interference at an External Node," NRL/FR/5521- -20-10,401, Naval Research Laboratory, https://apps.dtic.mil/sti/pdfs/AD1114565.pdf, November 6, 2020.

3. R. Wattenhofer and A. Zollinger, "XTC: A Practical Topology Control Algorithm for Ad-hoc Networks," Proceedings of the 18th International Parallel and Distributed Processing Symposium, 2004. Proceedings. (IEEE), 2004, p. 216.

4. S. Ghosh, K. Lillis, S. Pandit, and S. Pemmaraju, "Robust topology control protocols," Proceedings of the International Conference On Principles Of Distributed Systems (Springer), 2004, pp. 94–109.

5. G. F. Riley and T. R. Henderson, "The ns-3 network simulator," in *Modeling and tools for network simulation*, pp. 15–34 (Springer, 2010).

6. B. Winkel and A. Jessner, "Spectrum Management and Compatibility Studies with Python," *Advances in Radio Science* **16**, 177–194 (Sept. 2018), doi:10.5194/ars-16-177-2018.

7. M. Lacage and T. R. Henderson, "Yet Another Network Simulator," *Proceeding from the 2006 workshop on ns-2: the IP network simulator - WNS2 06* (2006), doi:10.1145/1190455.1190467.

8. J. Macker, "Simplified Multicast Forwarding (RFC 6621)," *Internet Engineering Task Force (IETF) Experimental Internet Standard* (2012).

9. T. Clausen and P. Jacquet, "Request For Comments (RFC) 3626: Optimized link state routing protocol (OLSR)," *Internet Engineering Task Force (IETF) Internet Standard* (2003).

10. P. Gupta and P. R. Kumar, "The capacity of wireless networks," *IEEE Transactions on information theory* **46**(2), 388–404 (2000).

11. N. Fan and J. P. Watson, "Solving the Connected Dominating Set Problem and Power Dominating Set Problem by Integer Programming," *Lecture Notes in Computer Science* pp. 371–383 (2012), ISSN 1611-3349, doi:10.1007/978-3-642-31770-5_33. URL http://dx.doi.org/10.1007/978-3-642-31770-5_33.

12. C. E. Miller, A. W. Tucker, and R. A. Zemlin, "Integer Programming Formulation of Traveling Salesman Problems," *Journal of the ACM (JACM)* **7**(4), 326–329 (Oct 1960), ISSN 1557-735X, doi:10.1145/321043.321046. URL http://dx.doi.org/10.1145/321043.321046.

13. "CVXPY Website." URL https://www.cvxpy.org/.

14. "Github coin-or branch-and-cut (cbc) solver website." URL https://github.com/coin-or/Cbc.

15. A. Ouni, H. Rivano, F. Valois, and C. Rosenberg, "Energy and Throughput Optimization of Wireless Mesh Networks With Continuous Power Control," *IEEE Transactions on Wireless Communications* **14**(2), 1131–1142 (2015), doi:10.1109/TWC.2014.2364815.